



## HOT DEFORMATION AND PROCESSING MAPS OF A PARTICULATE REINFORCED 7075AL/15%SiC METAL MATRIX COMPOSITE

\*Rajamuthamil selvan M and Ramanathan S

Department of Manufacturing Engineering, Annamalai University, Annamalai Nagar, TamilNadu - 608002, India.

### ABSTRACT

The mechanical response of a 7075/SiC/15% metal matrix composite is investigated by means of hot compression test. The flow stress curves obtained in temperature and strain rate ranges of 300 - 500 °C and 0.001-1.0 s<sup>-1</sup>, respectively in order to achieve the processing map of the studied material following the Dynamic Material Model. All zones of flow instability studied through an optical microscope. Microstructural characterization studies conducted on the compressed composite samples using an optical microscope image analyzer, revealed safe domains of dynamic recrystallization, elongation and nonsafe domains of adiabatic shear bands, interfacial ductile-tearing failure (debonding) of SiC Particles. The observations performed in order to describe the behaviour of the material under hot forming operations in terms of material damage and microstructural modifications.

**Keywords:** MMC, Hot Compression, Processing Map, Dynamic Recrystallization.

### 1. Introduction

Aluminium (Al)-based metal-matrix composites (MMCs) have very low coefficient of thermal expansion and high strength, wear resistance and heat resistance when compared with conventional Al alloys. Al-MMCs can substitute for steel to some degree when reinforced with ceramic particulate materials such as SiC, Al<sub>2</sub>O<sub>3</sub>, B<sub>4</sub>C, and TiC. Consequently, they have great potential of application in defense and automotive industries [1, 2].

Metal-matrix composites have been aided by the development of reinforcement material, which provides either improved properties or reduced cost when compared to the existing monolithic materials [2]. Particulate-reinforced metal-matrices have attracted considerable attention on account of availability of a spectrum of reinforcement at competitive costs, successful development of manufacturing processes to produce metal-matrix composites with reproducible microstructures and properties, and availability of standard and near standard metal working methods, which can be utilized to form these materials.

Hot deformation is concerned with the extent to which a material plastically deforms during shaping at high temperatures without the occurrence of flow localization or fracture. One of the requirements for process modeling is knowledge of the material flow behavior for defining deformation processing maps that delineate “safe” and “nonsafe” hot working conditions. These maps show in the processing space, i.e. on the axes

of temperature and strain rate, the processing conditions for stable and unstable deformation. The ultimate objective is to manufacture components with controlled microstructure and properties, without macro or microstructural defects, on a repeatable basis in a manufacturing environment. Hitherto, processes are developed using trial and error techniques which are expensive as well as time consuming and may not always lead to a successful solution or optimization. In recent years, the trial and error techniques are replaced by modeling techniques, which are developed on the basis of science based principles.

Frost and Ashby [3] were the first to attempt the materials response in the form of deformation mechanism map in which the emphasis has been essentially on the creep mechanisms applicable to lower strain rates. These maps are very useful for alloy design. Considering strain rate as one of the direct variable and temperature as the other, Raj [4] extended the concept of Ashby's maps to construct a processing map considering two different fracture nucleating mechanisms and calculated the limiting conditions for avoiding the microstructural damage. They are (i) cavity formation at hard particles in a soft matrix occurring at lower temperatures and higher strain rates, and (ii) wedge cracking at grain boundary triple junctions occurring at higher temperatures and lower strain rates. At very high strain rates, a regime representing adiabatic shear band formation was considered. In principle, there is always a region which may be termed “safe” for processing where neither of the two damage mechanisms nor adiabatic shear band formation occurs.

\*Corresponding Author - E-mail: rajanarmi@yahoo.co.in

The processing map technique has been widely used to understand the hot workability of many materials in terms of microstructural processes operating over a range of temperatures and strain rates [5]. The input to generate a processing map is the experimental data of flow stress as a function of temperature, strain rate and strain. As the map generated will be only as good as the input data, it is important to use accurate, reliable and yet simple experimental technique for generating them. In general, the material starts “flowing” or deforming plastically when the applied stress (in uniaxial tension without necking or in uniaxial compression without bulging) reaches the value of the flow stress. While hot tensile, hot torsion or hot compression testing techniques may be used for this purpose, hot compression test has decisive advantages over others.

First of all, in a compression test on a cylindrical specimen, it is easy to obtain a constant true strain rate using an experimental decay of the actuator speed. It is convenient to measure the adiabatic temperature rise directly on the specimen and conduct the test under isothermal conditions.

The aim of the present investigation is to study the hot compressive behavior of 7075 Al/15% SiCp composite was examined by compressive tests. The processing maps were constructed on the basis of the variations of power dissipation efficiency and instability parameters with temperature and strain rate. Subsequently identify various microstructural mechanisms and domains of safe and unsafe regions through microstructure observations. The optimum workability was designed by the processing maps.

The technique of processing maps is based on the dynamic materials model, the principles of which are described earlier [6, 7]. Briefly, the work-piece undergoing hot deformation is considered to be a dissipator of power and the total power dissipated instantaneously is given by

$$P = \int_0^{\dot{\epsilon}} \sigma \cdot d\dot{\epsilon} + \int_0^{\sigma} \dot{\epsilon} \cdot d\sigma = G + J \quad (1)$$

Where  $\sigma$  is the flow stress and  $\dot{\epsilon}$  is the strain rate. In terms of physical systems terminology, the first integral is called G content representing deformation heat and the second one a J co-content, which is a complementary part of G content, representing microstructural dissipation. The strain rate sensitivity (m) of flow stress is the factor that partitions power between deformation heat and microstructural changes since:

$$\frac{dJ}{dG} = \frac{\dot{\epsilon} \cdot d\sigma}{\sigma \cdot d\dot{\epsilon}} = \frac{\dot{\epsilon} \sigma d \ln \sigma}{\sigma \dot{\epsilon} d \log \dot{\epsilon}} \approx \frac{\Delta \log \sigma}{\Delta \log \dot{\epsilon}} = m \quad (2)$$

The efficiency of power dissipation ( $\eta$ ) occurring through microstructural changes during deformation is derived by comparing the non-linear power dissipation occurring instantaneously in the work-piece with that of a linear dissipater ( $m = 1$ ) and is given by

$$\frac{\Delta J / \Delta P}{(\Delta J / \Delta P)_{linear}} = \frac{m / (m + 1)}{1/2} = \frac{m}{m + 1} \equiv \eta \quad (3)$$

The power dissipation map represents the three-dimensional variation of efficiency with temperature and strain rate which is generally viewed as an iso-efficiency contour map. Further, the extreme principles of irreversible thermodynamics as applied to continuum mechanics of large plastic flow are explored to define a criterion for the onset of flow instability given by the equation for the instability parameter  $\xi(\dot{\epsilon})$

$$\xi(\dot{\epsilon}) = \frac{\delta \ln (m / m + 1)}{\delta \ln \dot{\epsilon}} + m < 0 \quad (4)$$

In simple terms, the material will exhibit flow instability if the rate of internal entropy production generated by the system during hot deformation is lower than that imposed by the applied processing parameters. The variation of the instability parameter as a function of temperature and strain rate represents an instability map which delineates regimes of instability where  $\xi$  is negative.

A superimposition of the instability map on the power dissipation map gives a processing map which reveals domains (efficiency contours converging towards a peak efficiency) where individual microstructural processes dominate and the limiting conditions for the regimes (bounded by a contour for  $\xi = 0$ ) of flow instability. Processing maps help in identifying temperature–strain rate windows for hot working where the intrinsic workability of the material is maximum (e.g. dynamic recrystallization (DRX) or super plasticity) and also in avoiding the regimes of flow instabilities (e.g. adiabatic shear bands or flow localization) or cracking. The processing map technique has been used earlier to study the hot deformation mechanisms in Al and its alloys [6, 8-9] including dynamic recrystallization (DRX) and flow instabilities.

The standard kinetic rate equation relating the flow stress ( $\sigma$ ) to strain rate ( $\dot{\epsilon}$ ) and temperature (T) is given by [10]:

$$\dot{\epsilon} = A \sigma^n \exp (-Q/RT) \quad (5)$$

Where  $A$  = constant,  $n$  = stress exponent,  $Q$  = activation energy, and  $R$  = gas constant. The rate-controlling mechanisms are identified on the basis of the activation parameters  $n$  and  $Q$ .

## 2. Experimental Studies

Stir casting technique was used to fabricate 7075Al alloy reinforced with 15% volume fraction of silicon carbide Composites. The matrix material was 7075 Aluminium Alloy (Composition in wt% Cu 1.66, Mg 2.10, Si 0.14, Mn 0.21, Fe 0.40, Cr 0.18, Zn 5.67, Ti 0.01 and rest Al) and the reinforcement was  $\text{SiC}_p$  with average size of  $5\mu\text{m}$ . The aluminium alloy was melted by using an Electric Furnace. Preheated  $\text{SiC}_p$  ( $250^\circ\text{C}$ ) was added to the melt and mixed by using a rotating impeller in Argon environment and poured in permanent mould. The cast billets were soaked in the temperature of  $400^\circ\text{C}$  for 30 minutes and hot extruded. The cylindrical specimens of dimensions, 10 mm in diameter and 10 mm in Height were machined from the extruded rods.

The hot compression tests [11] were performed on a 10T servo controlled universal testing machine for different strains (0.1 – 0.5), strain rates ( $0.001\text{s}^{-1}$  -  $1.0\text{s}^{-1}$ ) and temperatures ( $300$  -  $500^\circ\text{C}$ ). Temperature of the specimen was monitored with the aid of a chromel/alumel thermocouple embedded in a 0.5mm hole drilled half the height of the specimen as stated by Prasad Y.V.R.K. et al[12]. The thermocouple was also used for measuring the adiabatic temperature rise in the specimen during deformation.

The specimens were effectively lubricated with graphite and deformed to a true strain of 0.5. After compression testing, the specimens were immediately quenched in water and the cross section was examined for microstructure. Specimens were deformed to half of the original height. Deformed specimens were sectioned parallel to the compression axis and the cut surface was prepared for metallographic examination.

Specimens were etched with Keller's solution. The microstructure of the specimens was obtained through Versamet 2.0 optical microscope with Clemex vision Image Analyser and mechanism of deformation was studied. Using the flow stress data, power dissipation efficiency and flow instability were evaluated for different strain rates, temperatures at a constant strain of 0.5. The processing maps were developed for 0.5 strains for 7075Al/15%  $\text{SiC}_p$  composites.

## 3. Results and Discussion

Adiabatic temperature rise during high strain rate testing was measured and the flow stress was corrected for the temperature rise. The specimens were compressed to 50% of their initial height and the

load–stroke curves obtained in the hot compression were converted in to true stress–true plastic strain curves by subtracting the elastic portion of the strain and using the standard equations for the true stress and true strain calculations. The values of the efficiency parameter ( $\eta$ ) and the strain rate sensitivity parameter ( $m$ ) to use the instability condition [13] are determined from the flow stress test data of the material.

### 3.1. Flow behavior

Flow stresses to divide the characteristics of metal flows occurred for dynamic recovery and recrystallization, counting initial austenite grain size obtained from numerous experiments.

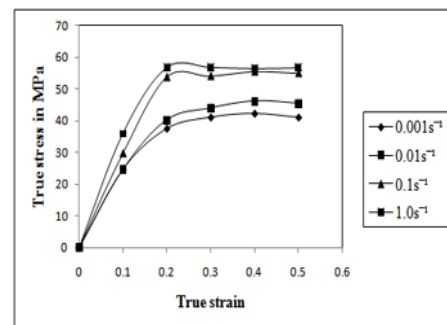
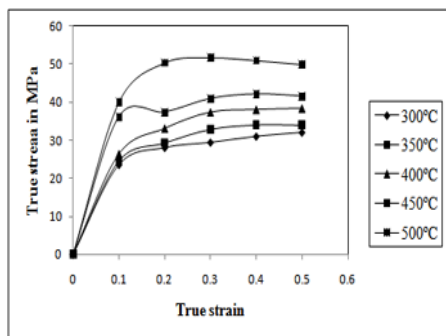


Fig. 1 The Flow Curves for Different a Strain Rates at Constant Temperature of  $400^\circ\text{C}$

The typical stress–strain curves are obtained at  $400^\circ\text{C}$  recorded at various true strain rates are shown in Fig 1. The representative temperature  $400^\circ\text{C}$  corresponds to peak domain temperatures. The flow curve corresponding to the centre of the plateau domain ( $400^\circ\text{C} / 0.01\text{s}^{-1}$ ) exhibits initial flow softening on reaching a single peak stress, followed by steady state flow. On the other hand, the flow curves of its neighborhood conditions exhibit oscillations (multiple peaks). In many materials, such flow features have been interpreted to be the result of dynamic restoration processes (DRY and DRX) [14]. These involve formation and growth of dislocation cells.

Typical flow stress strain curves for composite deformed at  $0.1\text{ s}^{-1}$  and different temperatures are shown in Fig 2. Comparing these curves, it is evident that the flow stress is a sensitive function of temperature and decreases markedly with increasing temperature. However, there appears to be little effect from strain rate on the stress strain behaviour at strain rates over the  $0.01\text{ s}^{-1}$  range, except for specimens deformed at room temperature. At all temperatures, the plastic true strain of the fracture point is over 0.4 for each strain rate. This means that the material is highly deformable by compression within this temperature range.

The differences in experimental temperature resulted in differences not only in the flow stress but also in the strain hardening rate. At temperatures below 350°C, strain hardening is stronger than at temperatures above 500°C. Also, higher temperature tests exhibit a more homogeneous deformation than room temperature tests. At constant strain rate, the decrease in the hardening rate with temperature is probably related to an increase in mobile dislocation density as well as to an annihilation of total dislocation density. Thus, the change of the work-hardening rate associated with the variation of dislocation density will be reflected in the plastic flow resistance [10].



**Fig. 2 The Flow Curves for Different Temperatures at Constant Strain Rate of 0.1s-1**

As mentioned above, strain rate and temperature affect the flow response of the tested composites. This phenomenon has been observed in many materials [8-10]. Typically, as the strain rate increases, there is increased strength and decreased ductility. However, increases in the test temperature typically have the opposite effect.

Flow stress decreases dramatically with temperature. This results from the effect of thermal Activation on the overcoming of dislocation flow barriers as the temperature is increased. The high-temperature flow resistance is controlled only by the thermal softening rate [10]. As the temperature increases the strengthening effect of SiC particles is considerably diminished.

### 3.2. Microstructures analysis

The approach of processing maps has been found [15] to be beneficial in arriving at optimum processing parameters and in avoiding microstructural defects including flow instabilities. A processing map is obtained by the superimposition of the variation of the efficiency of forming parameter with temperature and strain rate and the variation of instability parameter as a function of the same variables [6]. The input to generate a

processing map is the experimental data of flow stress ( $\sigma$ ) as a function of temperature ( $T$ ), strain rate ( $\dot{\epsilon}$ ) and strain ( $\epsilon$ ).

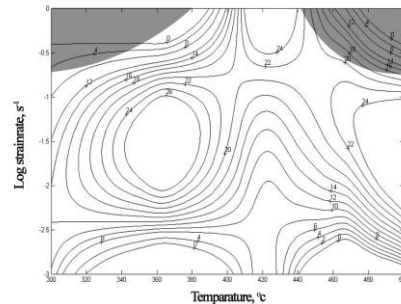


**Fig. 3 Processing Map for 7075Al/15% SiCp Composites at 0.5 Strain**

The processing map obtained at a strain of 0.5 (steady state) is shown in Fig 3. The contours represent efficiency of power dissipation marked as percent and the thick line separates the stable and unstable regions. The map exhibits the domain is obtain at the temperature and strain rate ranges are 345–385 °C and 0.01–0.1 s<sup>-1</sup> with a peak efficiency of about 26% at 365 °C and 0.05 s<sup>-1</sup>.

The stable efficiency value as a function of strain indicates that the power dissipation is through equilibrium microstructural processes occurring during deformation, namely the dynamic restoration processes such as DRX, DRV and extended DRV. These processes involve in situ dislocation generation and annihilation with deformation, which attain equilibrium state with strain. As these processes are less effective in dissipating power compared to fracture processes, the efficiency associated with the plateau domain is comparatively less [14].

Microstructure analysis reveal that the microstructures have been replaced (Fig 4) by recrystallized structure. Processing parameter viz. strain rate temperature has a very strong influence of workability of the material as well as mechanical property of the product. The various mechanism operating at various processing conditions are responsible for each variation in mechanical properties. For example of DRX or DRV would result enhanced ductility of the material [16]. The properties of a metal are strongly influenced by its microstructural features like the grain size and the grain/sub-grain orientation / mis-orientation.

The mechanisms of microstructure evolution during thermo-mechanical processing include strain hardening, recrystallization and grain growth. The stored energy was established early as one of the important driving forces behind recrystallization. Recrystallization is a further restoration process wherein new dislocation

free grains are formed within the deformed microstructure. Recrystallization may also take place during deformation at elevated temperatures and this is termed as dynamic recrystallization.

The dynamic recrystallized zone obtained at a temperature of 350 °C and a strain rate of 0.1 s<sup>-1</sup> for 0.5 strain is shown in Fig. 4. Similarly grain elongation obtained at temperature of 350 °C and a strain rate of 0.01 s<sup>-1</sup> is shown in Fig 5.

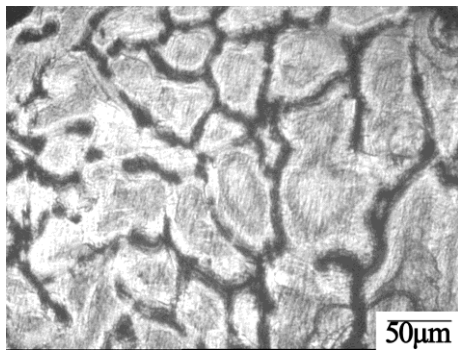


**Fig. 4 Dynamic Recrystallization at 400°C at a Strain Rate of 0.1s-1**

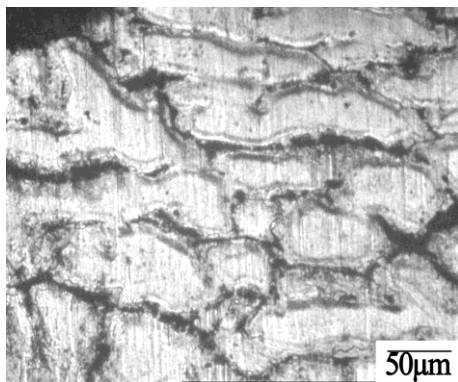


**Fig. 5 Grain Elongation at 400°C and at a Strain Rate of 0.01s-1**

Another area of discussions has been whether or not aluminum exhibits DRX. Neither the flow curves exhibit flow softening features nor do the frozen microstructures show significant DRX feature such as nuclei at the prior grain boundaries and grain refinement. G. Ganesan et al [17] opined that DRX does not occur in aluminium in view of its high SFE and the primary softening mechanism is only dynamic recovery though exceptions have been made for very high purity aluminium and some particle containing alloys. While the basis for these exceptions has not been clearly understood, several different DRX mechanisms have been proposed and these include continuous DRX in the

initial stages of super plasticity and ‘geometric’ DRX both of which refine grains size. These conclusions are based on the measurement of flow stress under dynamic deformation conditions and can be, therefore, considered to the more reliable than those based on frozen microstructure.

The flow instability occurs in two different zones. At higher strain rate range of 1.0 s<sup>-1</sup> between temperature ranges of 300 - 380 °C the instability has occurred. The second zone has occurred at higher strain rate range of 1.0 s<sup>-1</sup> between temperatures of 450 - 500 °C.

Localization may occur in two modes. In the first mode of localization, discontinuous deformation often localizes in narrow zones and the neighboring regions remain intact. Factors such as material compositions, boundary conditions and type of loading may affect localization. A material can fail due to the formation and growth of micro cracking at randomly distributed locations.

In the second mode localization may result in motions along preferential directions called shear bands and can lead to extensive deformation and failure [18]. Localization usually occurs at peak load but some times it may occur before reaching peak. Beyond peak the material may experience softening or degradation in its load carrying capacity, but still continue to carry reduced load compared to peak load while growth and coalescence of micro cracks continue during the falling region of the curve. Finally the micro crack growth leads to a macro crack and fracture. At higher strain rates, heat generated due to local temperature rise by plastic deformation is not conducted away to the cooler regions of the body since the available time is too short. The flow stress in deformation will get lowered and further plastic flow will be localized. The band gets intensified and nearly satisfies adiabatic conditions. Such bands are called adiabatic shear bands, which exhibit cracking, recrystallization along macroscopic shear planes [18].

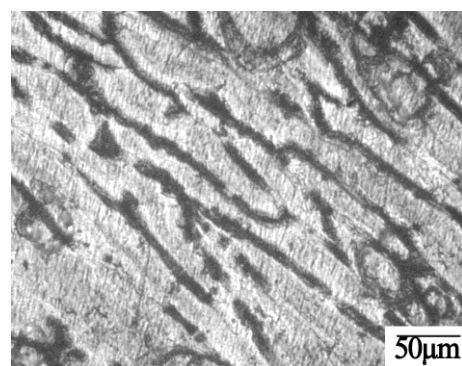


**Fig. 6 Shear Band Formation at 300°C and at a Strain Rate of 1.0s-1**

Fig. 6 represents the formation of shear bands at a high strain rate of  $1.0 \text{ s}^{-1}$  and a temperature of  $300 \text{ }^\circ\text{C}$  for 0.5 strains.

The micro cracks, initiating in the SiC/Al interface and propagating in the matrix, generated the pulling-out of SiC particles. In the Al matrix near the plastic pits there are some small dimples displaying the typical ductile fracture of the matrix alloy. At the same time, the presence of dimples at the SiC/Al interface reveals that the bonding between matrix and reinforcements is strong enough so that high strain is needed to break the interface and initiate the void sheet coalescence mechanism for dimple formation [19] Pulled out SiC particles were covered with the Al matrix, which

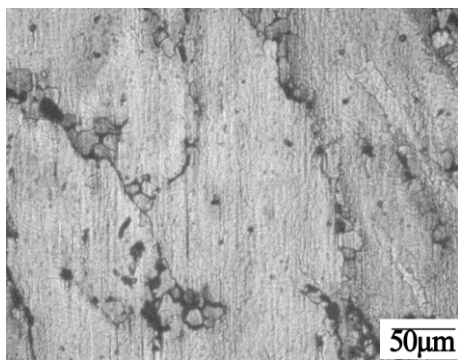


**Fig. 7 Interfacial Ductile-Tearing Failure at  $500^\circ\text{C}$  and at a Strain Rate of  $1.0\text{s}^{-1}$**

shows the ductile-tearing failure along the SiC/Al interface. This ductile-tearing failure is different from the commonly observed interfacial decohesion that will result in a much smooth fracture surface. The interfacial ductile-tearing failure observed here may be attributed to the enhanced SiC/Al interfacial bonding owing to the prolonged diffusional time of the constituent elements in the sintering process and to the presence of the highly gradient alloying element area vicinal to the SiC/Al interface. Fig 7 represents interfacial ductile-tearing failure at a high strain rate of  $1.0 \text{ s}^{-1}$  and a temperature of  $450 \text{ }^\circ\text{C}$  for 0.5 strains. Although the SiC particles distributed homogeneously in the matrix, the existence of few clustered SiC particles with lower plastic deformation has been found in the fracture surface of the composites. In these regions, the distance between a SiC particle and its neighbors was short, resulting in the high local stress concentration which decreased the ductility and fracture toughness of the composites. Consequently, the few clustered SiC particles became the major sources of cracks in the composites. The matrix strength, SiC/Al matrix interfacial cohesion, the particle size and the uniformity of SiC particles have played important roles in fracture of the composites [20].

## 4. Conclusion

Hot compression tests were performed on Al/15% SiC composites produced through Stir casting technique. The flow stress was evaluated for a temperature range of  $300 - 500 \text{ }^\circ\text{C}$  and a strain rate range of  $0.001 - 1.0 \text{ s}^{-1}$ . The power dissipation efficiency and instability parameters were evaluated and processing maps were constructed for 0.5 strains. The optimum domains and instability zone were obtained for the material. The domains for hot working significantly differ from that of pure aluminium. The microstructure evaluation leads to adiabatic shear band formation and interfacial ductile-tearing failure which led to flow instability of the composites. The super plastic deformation and dynamic recrystallization zones correspond to optimum working regions were identified. The ductile-tearing mechanism of SiC/Al interfaces are of the main fracture modes of the composites. The microstructures and deformation behavior of the composites strongly depend on the matrix properties, the presence of reinforcements and preparation process.

## References

1. Fevzi Bedir (2007), "Characteristic Properties of Al-Cu-SiCp and Al-Cu-B4Cp Composites Produced by Hot Pressing Method under Nitrogen Atmosphere", *Materials Design*, Vol.28, 1238-1244.
2. Ali Kalkanl, and Sencer Yilmaz (2008), "Synthesis and Characterization of Aluminum Alloy 7075 Reinforced with Silicon Carbide Particulates", *Materials Design*, Vol.29, 775-780.
3. Frost H J and Ashby M F (1982), "Deformation Mechanism Maps, the Plasticity and Creep of Metals and Ceramics", London: Pergamon Press.
4. Raj R (1981), "Development of a Processing Map for Use in Warm Forming and Hot Forming Processes", *Metallurgical and Materials Transactions A*, Vol. 12(6), 1089-1097.
5. Srinivasan N, Prasad Y V R K and Ramarao P (2008), "Hot Deformation Behaviour of Mg-3Al Alloy- a Study using Processing Map", *Material Science and Engineering: A*, Vol. 476(1-2), 146-156.
6. Cavaliere P, Cerri E and Leo P (2004), "Hot Deformation and Processing Maps of a Particulate Reinforced 2618/Al<sub>2</sub>O<sub>3</sub>/20p Metal Matrix Composite", *Composites Science and Technology*, Vol. 64(9), 1287-1291.
7. Prasad, Y V R K (2003), "Processing Maps - A Status Report", *Journal of Materials Engineering and Performance*, Vol. 12(6), 638-645.
8. Spigarelli S, Cerri E, Cavaliere P and Evangelista E (2002), "An Analysis of Hot Formability of the 6061+20% Al<sub>2</sub>O<sub>3</sub> Composite by Means of Different Stability Criteria", *Materials Science and Engineering: A*, Vol.327, 144-154.

9. Narayana Murty S V S, Nageswara Rao B and Kashyap B P (2005), "On the Hot Working Characteristics of 2014 Al–20 Vol% Al<sub>2</sub>O<sub>3</sub> Metal Matrix Composite", *Journal of Materials Processing Technology*, Vol. 166, 279–285.
10. Woei-Shyan Lee, Chi-Feng Lin, and Sen-Tay Chang (2000), "Plastic Flow of Tungsten-Based Composite under Hot Compression", *Journal of Materials Processing Technology*, Vol. 100, 123–130.
11. Lin Y C, Ming-Song Chen, and Jue Zhong (2008), "Prediction of 42CrMo Steel Flow Stress at High Temperature and Strain Rate", *Mechanics Research Communications*, Vol. 35(3), 142–150.
12. Prasad Y V R K and Rao K P (2005), "Processing Maps and Rate Controlling Mechanisms of Hot Deformation of Electrolytic Tough Pitch Copper in the Temperature Range 300-950° C", *Materials Science and Engineering: A*, Vol. 391,141–150.
13. Seshacharyulu T, Medeiros S C, Morgan J T, Malas J C, Frazier W G and Prasad Y V R K , (2000), "Hot Deformation and Microstructural Damage Mechanisms in Extra Low Interstitial (ELI) Grade Ti-6Al- 4V", *Materials Science and Engineering: A*, Vol. 279, 289–299.
14. Jagan Reddy G, Srinivasan N, Amol A , Gokhale B P , and Kashyap (2009), "Processing Map for Hot Working of Spray Formed and Hot Isostatically Pressed Al–Li Alloy (UL40)", *J Journal of Materials Processing Technology*, Vol. 209, 5964–5972.
15. Prasad Y V R K and Sasidhara S (1997), "Hot Working Guide: A Compendium of Processing Maps", *ASM International, Materials Park, OH*,
16. Sivaprasad P V , Venugopal S , SridharVenugopal, Maduraimuthu V , Vasudevan M , Mannan S L , Prasad Y V R K and Chaturvedi R C (2009), "Validation of Processing Maps for a15Cr-15Ni-2.2Mo-0.3Ti Austenite Stainless Steel Using Hot Forging and Rolling Tests", *Journal of Materials Processing Technology*, Vol. 132, 262-268.
17. Ganesan G, Raghukandan K, Karthikeyan R and Pai B C (2004), "Development of Processing Maps for 6061 Al/15% SiCp Composite Material", *Materials Science and Engineering: A*, Vol. 369, 230–235.
18. Ramanathan S, Karthikeyan R and Manoj Gupta (2007), "Development of Processing Maps for Al/SiCp Composite using Fuzzy Logic", *Journal of Materials Processing Technology*, Vol. 183,104–110.
19. Ceschini,L, Minak,G., and Morri,A.,2009, "Forging of the AA2618/20 vol.% Al<sub>2</sub>O<sub>3</sub>p Composite: Effects on Microstructure and Tensile Properties", *Composite Science and Technology*, Vol. 69, 1783–1789.
20. Cheng NP, Zeng SM and Liu Z Y (2008), "Preparation, Microstructures and Deformation Behavior of SiCP/6066Al Composites Produced by PM Route", *Journal of Materials Processing Technology*, Vol.202, 27-36.

## Acknowledgement

The authors are grateful to The Department of Manufacturing Engineering, Annamalai University, Tamilnadu, India for the support rendered for the fabrication and testing of Composites.

